# SUPERNOVAE X-RAY ANALYSIS: FROM SWIFT TO SIBEX

An Undergraduate Research Scholars Thesis

by

MACIE ROBERTSON

Submitted to the LAUNCH: Undergraduate Research office at
Texas A&M University
in partial fulfillment of the requirements for the designation as an

UNDERGRADUATE RESEARCH SCHOLAR

Approved by
Faculty Research Advisor: Dr. Darren DePoy

May 2022

Major: Physics-Astrophysics, B.S.

# RESEARCH COMPLIANCE CERTIFICATION

Research activities involving the use of human subjects, vertebrate animals, and/or biohazards must be reviewed and approved by the appropriate Texas A&M University regulatory research committee (i.e., IRB, IACUC, IBC) before the activity can commence. This requirement applies to activities conducted at Texas A&M and to activities conducted at non-Texas A&M facilities or institutions. In both cases, students are responsible for working with the relevant Texas A&M research compliance program to ensure and document that all Texas A&M compliance obligations are met before the study begins.

I, Macie Robertson, certify that all research compliance requirements related to this Undergraduate Research Scholars thesis have been addressed with my Research Faculty Advisor prior to the collection of any data used in this final thesis submission.

This project did not require approval from the Texas A&M University Research Compliance & Biosafety office.

# TABLE OF CONTENTS

# ABSTRACT

Supernovae X-Ray Analysis: From Swift to SIBEX

Macie Robertson
Department of Physics and Astronomy
Texas A&M University

Research Faculty Advisor: Dr. Darren DePoy
Department of Physics and Astronomy
Texas A&M University

A supernova is an explosion of a stellar body at the end of its lifespan that creates shock waves that can sometimes emit X-rays. An X-ray is a form of radiation and light with a wavelength ranging from 0.5-2.5 Å that can be used to make constraints on the physics of the explosion and understand more about the nature of the supernova's environment. Previous X-ray emissions from supernovae have been observed by telescope systems such as the Roentgen Satellite (ROSAT), Chandra, and Swift. The data from these observations have been made available on databases such as the Swift X-Ray Telescope (XRT) Database and the Supernova X-Ray Database (SNaX). Count rates and upper limits for 18 different supernovae were measured using an online XRT analysis tool, converted to fluxes and luminosities, and plotted using Python. Analyses of these data sets will be useful in understanding what could be seen by a proposed future spacecraft SIBEX, the Shock Interaction/Breakout Explorer. SIBEX will be a satellite telescope that allows for detection of supernovae at the moment of explosion rather than in the days or months after explosion. This will allow for quicker observations, which will provide more time for scientists to make observations and expand human knowledge.

# DEDICATION

*To my late grandfather, Dr. David R Criswell, who inspired me with his studies in the astrophysical field, and all of my loving family members who have supported me along the way.*

# ACKNOWLEDGMENTS


## Contributors

I would like to thank my faculty advisor, Dr. Darren DePoy, and my project leader, Dr. Peter Brown, for their guidance and support throughout the course of this research.

Thanks also go to my friends and colleagues and the department faculty and staff for making my time at Texas A&M University a great experience.

Finally, thanks to my family for their encouragement, patience, and love.

The data used for Supernovae X-Ray Analysis: From Swift to SIBEX were provided by Dr. Peter Brown and NASA's Neil Gehrels Swift Observatory and were analyzed using an automated tool from the University of Leicester. The observations analyzed in Supernovae X-Ray Analysis: From Swift to SIBEX were triggered by Dr. Peter Brown and were obtained between 2018 and 2019.

All other work conducted for this thesis was completed by the student independently.

## Funding Sources

The work of Dr. Peter Brown was obtained and funded in part by a NASA/Swift project, "Supernova Key Project: Swift Response to New Transients." The student did not receive any funding.

# NOMENCLATURE

| | |
|---|---|
| SN | Supernova |
| SIBEX | Shock Interaction/Breakout Explorer |
| NASA | National Aeronautics and Space Administration |
| ADS | Astrophysics Data System |
| SNaX | Supernova X-ray Database |
| ROSAT | Roentgen Satellite |
| NGC | New Galaxy Catalog |
| XRT | X-Ray Telescope |
| MJD | Modified Julian Date |
| MET | Mission Elapsed Time |
| GRB | Gamma Ray Burst |

# 1. INTRODUCTION

This section will introduce what a supernova is, types of supernovae, X-Rays and Compton Scattering, and previous observations that have been made by different astronomical groups and telescope systems.

## 1.1 Supernova and Types

### *1.1.1 What is a Supernova?*

One of the most violent known phenomena to occur in our universe is a supernova, which is the explosion of a star at the end of its lifespan. These explosions create radiation and shock waves, which can emit X-Rays by the forward and reverse shockwaves heating the debris from the explosion. Supernovae are typically detected by telescopes within a few days of exploding, as it takes time after the supernova explodes for it to become bright enough to be detected by the telescope. [1] SIBEX, the anticipated future mission, hopes to cut down the time it takes to detect a supernova so that it can be discovered at the moment of explosion, rather than in the days following.

### *1.1.2 Types of Supernovae*

There are two main classifications of supernovae, Type I and Type II. The primary difference between these two types is that Type I supernovae do not show clear evidence of hydrogen in the debris caused by the explosion, whereas Type II do. Within Type I, there are 3 different sub-types, Type IA, Type Ib, and Type Ic. Type Ib and Ic are similar to Type II, as they all are results of a massive star exploding. However, they differ in that the progenitor of a Type II retains the hydrogen envelope that surrounded the star before exploding, but Type Ib and Ic do not. Type IA supernovae are results of white dwarf stars that exploded and also lost their hydrogen envelope well before explosion.

## 1.2 X-Rays and Compton Scattering

### *1.2.1 What is an X-Ray?*

X-Rays are a form of radiation or light that can be emitted by the shock waves produced during a supernova explosion. Wavelength of X-Rays ranges from 0.5-2.5 Å, which is shorter than Gamma rays and longer than Ultraviolet light. X-rays are produced in extremely high temperatures of millions of degrees Celsius. While X-ray emissions alone rarely reveal locations of supernova explosions, observing these emissions can help reveal more about the nature of stars before, during, and after explosion [2]. There are a few exceptional cases of X-ray detections leading to the discovery of a supernova, such as GRB060218/SN2006aj, which will be discussed later in this paper.

### *1.2.2 Compton Scattering*

X-Ray photons, which are essentially bundles of energy that behave as particles, can collide with electrons and experience a process known as Compton scattering, which occurs when the electron's energy is higher than the incident photon's, which in turn boosts the photon's energy. [2]. Compton scattering is the dispersion of X-Rays from electrons that provides evidence for particle-like behavior of waves. This scattering causes a wavelength shift that can be found using Compton's formula shown in Eq. 1.1. [3]

$$\lambda_f - \lambda_i = \Delta\lambda = \frac{h}{m_e c}(1 - cos\theta) \qquad \text{(Eq. 1.1)}$$

Compton scattering is important in the discussion of not only supernovae, but also black holes, which contain high temperatures and dense matter and are known to produce X-Rays [2].

## 1.3 Previous Observations

Previous observations of X-ray bursts by supernovae days after explosion by Swift, Chandra [4], and ROSAT [5], which are different supernovae observatories, can be used to predict future emissions that could be measured at the moment of explosion by SIBEX. SIBEX is an important

future goal, as it would allow for earlier observation of X-ray emissions by supernovae, which would help determine and confirm the causes and effects of these emissions.

### *1.3.1 ROSAT Observations*

Observations made by ROSAT are primarily based on supernovae occurring in galaxies with a New Galaxy Catalog, or NGC, number and show the upper limits on X-ray emissions of type IA and type II supernovae. NGC galaxies are convenient to look at because they are relatively close and ROSAT is not as sensitive as other systems. Early data showed that type II were the only ones that were detected as X-ray sources, and confirmed that Compton scattering of gamma rays produced the observed X-rays [5]. ROSAT was also essential in early observations of supernovae, such as SN1993J. This observatory was able to detect soft X-rays emitted by SN1993J just six days after outburst. This was one of the quicker detections made at the time [6].

### *1.3.2 Swift and Chandra Observations*

Swift and Chandra are often used together when observing supernovae. Swift is faster and more precise, but Chandra is better at creating detailed images of the supernova and its surroundings. When used together, the images produced by Chandra can help with interpretation of observations made by Swift. For example, these two systems were used, among many others, to discover and observe SN2018ivc in NGC2068. The observations made by Chandra are slightly more significant than those made by Swift, as Swift's angular resolution is must lower than Chandra's, which can make it hard to distinguish the supernova from its host galaxy. This supernova was very unusual, as its light curve was found to change rapidly. X-ray emissions were also fitted to two different background source options, and the results of each were consistent with each other within a reasonable amount of uncertainty [7]. Swift and Chandra were also used to observe SN2013ej. Cosmic ray acceleration efficiency from X-ray emissions was determined by Inverse Compton scattering, and these X-ray emissions were clearly detected and then modeled to show flux and luminosity of the supernova [4].

### *1.3.3 Kronos Observational Database*

SNaX is an astronomical database that was established in 2017 by the University of Chicago in collaboration with NASA, the National Aeronautics and Space Administration. Data is collected from numerous observatories, including Swift and Chandra, and uploaded to the user-friendly database accessible online. Several specifications can be made while making a query, such as sorting observations by galaxy, instrument of measurement, and even supernova age. Most of this project's data will be Swift-XRT, or X-Ray Telescope and measurements directly from Swift. In the future, we hope to use data found on this database [8] and compare it to the Swift data analyzed in this paper.

# 2. METHODS

The supernovae that were chosen to be analyzed from Swift's database were observed between April 2018 and March 2019 during a Swift Guest Investigator Program, "Swift Response to New Transients." Swift was triggered to make observations as soon as a new transient was discovered within a distance of 35 Megaparsecs (Mpc), rather than the typical method of waiting for a supernova to be classified through spectroscopy. The observations for each supernova were spaced one day apart for three days, with exposure times of 3000 seconds each. After determining which supernovae would be observed, I searched them by name, coordinates, and target ID on the database, and the data were binned by observation ID. I then downloaded the data from these observations from Swift's XRT database using an automated pipeline[1] to provide data.

The resulting downloaded data files included values for detection date and time, time since detection, estimated time measurement error, count rate or upper limit, approximate source error, and observation ID. The primary values used for this project were time since detection and count rate/upper limit. Count rate is a measurement of the number of photons produced by a supernova per second, and upper limits are approximations for highest possible values of count rates. Count rates (or upper limits) were converted to fluxes, which were then converted to luminosities using a defined Python function. This conversion essentially turns the count rate into an energy, which provides a rate from a given source rather than just a value from a detector. In **Section 3: Results**, the results of plotting these data sets against time since each detection date using Matplotlib can be found, as well as a table of the calculated values.

## 2.1 Equations for Conversion

The following equations were used to convert count rates to luminosities in the X-rays. Luminosity is a measurement of the energy released from the source of explosion and is an intrinsic property of a star. Flux is non-intrinsic, so it varies depending on the point of observation, whereas luminosity does not. This is why luminosity is preferred over flux.

[1] https://www.swift.ac.uk/user$_objects/$

$$\textit{distance in pc} = 10 \cdot \sqrt{100^{Modulus/5}} \quad \text{(Eq. 2.1)}$$

$$\textit{distance in cm} = \textit{distance in pc} \cdot 3.086e18 \quad \text{(Eq. 2.2)}$$

Eq. 2.1 shows the conversion of a distance modulus to a distance in parsecs. A distance modulus is the logarithmic scale of the difference between apparent and absolute magnitudes, and it is usually used to describe extremely large distances that may not show a measurable parallax. The distance moduli were compiled from several different papers from the NASA's Astrophysics Data System (ADS) [9][10][11][12][13][14][15][16][17][18][19][20][21][22]. Eq. 2.2 shows the conversion of parsecs to centimeters, where 3.06e18 is the standard conversion factor.

$$flux = \textit{count rate} \cdot 5.61e - 11 \quad \text{(Eq. 2.3)}$$

Eq. 2.3 yields a flux using a given count rate. The factor of 5.61E-11 is an average flux/count rate factor that was calculated from tabulated values from [23].

$$Luminosity = 4\pi \cdot flux \cdot distance^2 \quad \text{(Eq. 2.4)}$$

Eq. 2.4 provides a value for luminosity in ergs/second using a given distance in square centimeters, calculated using Eq. 2.1 and Eq. 2.2, and a given flux, calculated using Eq. 2.3. Luminosity is an intrinsic property of a stellar object, meaning its value does not depend on the distance to the object. Flux is equivalent to luminosity per unit area and does depend on the distance to the object. Astronomers prefer to measure luminosity as opposed to flux because it is an intrinsic property that is independent of distance and can be compared to physical values and predictions.

$$\textit{Time since Discovery} = [(T_0 + T_{obs})/86400] + 51910 - T_{disc} \quad \text{(Eq. 2.5)}$$

Eq. 2.5 shows the calculation of the time that count rates were observed in MJD, or Mod-

ified Julian Date. In each SN data file, a $T_0$ was given in MET, or Mission Elapsed Time, as a reference time in seconds since MJD 51910. $T_{obs}$ is the time count rate was observed in seconds since the provided $T_0$. $T_0$ and $T_{obs}$ are added together and divided by 86400 to get a time in days. Then, 51910 is added to account for the conversion of MET to MJD. Finally, $T_{disc}$, or the time that the SN was discovered in MJD, is subtracted off to get the final time since discovery. Values for Time since Discovery for select observations and Detection Date of each SN can be found in **Table 3.1** and **Table 3.2** in the **Results** section of this paper.

## 2.2 Python Codes

### *2.2.1 Luminosity Calculation*

**Figure 2.1** below shows the code for reading in SN data from downloaded data files from Swift-XRT's database and converting count rates to luminosities. The first few lines of the code pull out and define the count rate from the data file. Then, a function is defined to convert distance moduli to units of parsecs and then to centimeters using Eq. 2.1 and Eq. 2.2. Another function is defined to convert count rate to flux using Eq. 2.3 and then flux to luminosity using Eq. 2.4. Finally, the end of the code generates a plot of the SN luminosity versus time since detection. This code was run using data from 18 different supernovae in total.

```
import numpy as np
import matplotlib.pyplot as plt

time, tpose, tnege, rate, ratepos, rateneg, obsid = np.loadtxt("SN2018hnacurve_plain.dat", skiprows=(13), unpack=True, dty

time = time.astype(float)
tpose = tpose.astype(float)
tnege = tnege.astype(float)
rate = rate.astype(float)
ratepos = ratepos.astype(float)
rateneg = rateneg.astype(float)

def Modulus_to_Distance(M):
    parsecs = 10*(100**(M/5))**(1/2)
    cm = parsecs*3.086e+18
    return cm

hna_dist = Modulus_to_Distance(30.11)

def CR_Flux_Luminosity(CR):
    answer = [] # to make your function array friendly, you have to first create an empty array that you will append to la
    number = 5.61E-11     # cr to flux conversion factor
    flux = (CR*number)
    distance = hna_dist
    luminosity = (flux*(distance**2)*4*3.14) # here you can make your equation
    answer.append(CR_Flux_Luminosity) # this is where you basically "save" the answers from your equation to that empty ar
    return luminosity # this is how your function knows what to output -- you are outputting those answers that you "saved

hna_lumi = CR_Flux_Luminosity(rate)

plt.plot(time,hna_lumi)
plt.title("Luminosity vs. Time for SN2018hna")
plt.xlabel("Time (s)")
plt.ylabel("Luminosity (ergs/s)")
```

Figure 2.1: Defining a Function to Convert Count Rate to Luminosity.

### *2.2.2 Time Caculation*

**Figure 2.2** below shows the calculation of the time that observations were made in units of days since discovery. Note that this is a defined function using Eq. 2.5, and this code was run for 18 different supernovae.

```
import numpy as np

time, tpose, tnege, rate, ratepos, rateneg, obsid = np.loadtxt("SN2018hnacurve_plain.dat", skiprows=(13), unpack=True, dtype=

time = time.astype(float)
tpose = tpose.astype(float)
tnege = tnege.astype(float)
rate = rate.astype(float)
ratepos = ratepos.astype(float)
rateneg = rateneg.astype(float)

time_array = np.array(time)
def t_since_disc(t):
    answer = []
    t_s = (t + 561997502.4006)
    t_d = t_s/86400
    t_disc = 58413
    MET_conv = 51910 - t_disc
    t_since_tdisc = t_d + MET_conv
    answer.append(t_since_disc)
    return t_since_tdisc
hna_time = t_since_disc(time_array)
```

Figure 2.2: Defining a Function to Convert Observation Time from Seconds to Days Since Detection

### *2.2.3 Overlaid Plots*

**Figure 2.3** displays the code used to superimpose plots of luminosity (with a solid dot indicating a detection and an upside-down triangle indicating an upper limit) versus time since detection. The output plot can be found in **Figure 3.2** in the **Results** section of this paper. A separate plot including only detections was made by eliminating the lines of code with "marker='v'" included, as these were supernovae with only upper limits. This plot can be found in **Figure 3.3** in the **Results** section of this paper.

```
plt.scatter(aoq_time,aoq_lumi, label='SN2018aoq')
plt.scatter(ivc_time,ivc_lumi, label='SN2018ivc')
plt.scatter(lei_time,lei_lumi, label='SN2018lei')
plt.scatter(bl_time,bl_lumi, label='SN2019bl')
plt.scatter(aoz_time,aoz_lumi, marker='v', label='SN2018aoz')
plt.scatter(avo_time,avo_lumi, marker='v', label='SN2018avo')
plt.scatter(bbl_time,bbl_lumi, marker='v', label='SN2018bbl')
plt.scatter(bsk_time,bsk_lumi, marker='v', label='SN2018bsk')
plt.scatter(bvt_time,bvt_lumi, marker='v', label='SN2018bvt')
plt.scatter(bwo_time,bwo_lumi, marker='v', label='SN2018bwo')
plt.scatter(gwo_time,gwo_lumi, marker='v', label='SN2018gwo')
plt.scatter(hna_time,hna_lumi, marker='v', label='SN2018hna')
plt.scatter(hrg_time,hrg_lumi, marker='v', label='SN2018hrg')
plt.scatter(abn_time,abn_lumi, marker='v', label='SN2019abn')
plt.scatter(ahd_time,ahd_lumi, marker='v', label='SN2019ahd')
plt.scatter(clr_time,clr_lumi, marker='v', label='SN2019clr')
plt.scatter(np_time,np_lumi, marker='v', label='SN2019np')
plt.scatter(yz_time,yz_lumi, marker='v', label='SN2019yz')
plt.title("Luminosity vs. Time")
plt.xlabel("Time (days since detection)")
plt.ylabel("Luminosity (ergs/s)")
ax = plt.subplot(111)
ax.legend(loc='center left', bbox_to_anchor=(1, 0.5), ncol=2)

plt.savefig("combined_lumi_time_plot.png")
```

Figure 2.3: Code to Plot Observed Luminosity vs Time for All 18 SN.

# 3. RESULTS

The following data showed that most of the supernovae were not detected. However, comparison of the upper limits to a known supernova showed that these limits were quite sensitive, and anything as luminous as these upper limits would be detected. Additionally, it can be seen that SN2018aoq, SN2018bwo, and SN2018ivc show observations well before explosion and, as a result, these detected X-rays are likely dominated by the host galaxy rather than the supernova. If there was less galaxy interference, these supernovae would likely not have so many observations before explosion. The resulting data is summarized as follows.

## 3.1 Tables of Count Rate, Flux, and Luminosity

**Table 3.1** below summarizes the results of converting upper limits for count rate to luminosity for 14 of the 18 selected supernovae.

Table 3.1: Count Rate and Luminosity Upper Limits

| SN Name | Observation Date (MM-DD-YYYY) | Days Since Discovery | Discovery Date (MJD) | Count Rate Upper Limit (photons/s) | Luminosity Upper Limit (ergs/s) |
|---|---|---|---|---|---|
| SN2018aoz | 05-15-2018 | 34.20 | 58210 | 1.7904e-02 | 5.4412e+40 |
| SN2018avo | 04-27-2018 | 2.27 | 58224 | 7.1996e-03 | 1.1273e+40 |
| SN2018bbl | 05-07-2018 | 3.93 | 58232 | 2.6252e-03 | 1.3363e+40 |
| SN2018bsk | 05-28-2018 | 3.24 | 58254 | 3.4132e-03 | 2.9370e+40 |
| SN2018bvt | 06-01-2018 | 1.63 | 58259 | 6.1469e-03 | 3.5269e+40 |
| SN2018bwo | 08-16-2015 | 1.300 | 58260 | 8.2353e-03 | 2.5493e+39 |
| SN2018gwo | 10-09-2018 | 1.74 | 58389 | 3.2247e-03 | 1.6567e+40 |
| SN2018hna | 01-25-2019 | 86.39 | 58413 | 2.8334e-03 | 2.1040e+39 |
| SN2018hrg | 11-11-2018 | 1.96 | 58422 | 4.0748e-03 | 2.5168e+38 |
| SN2019abn | 02-06-2019 | 6.53 | 58505 | 4.3789e-03 | 1.5708e+39 |
| SN2019ahd | 02-10-2019 | 2.55 | 58512 | 3.7567e-03 | 5.0298e+39 |
| SN2019clr | 04-09-2019 | 2.73 | 58570 | 3.6044e-03 | 4.8705e+38 |
| SN2019np | 01-29-2019 | 11.23 | 58492 | 5.2845e-03 | 3.8172e+40 |
| SN2019yz | 02-04-2019 | 5.50 | 58503 | 5.5172e-03 | 2.7572e+40 |

**Table 3.2** below summarizes the results of converting detections for count rate to luminosity for 4 of the 18 selected supernovae. These observations were the earliest after the discovery of each supernova.

Table 3.2: Count Rate and Luminosity Detections

| **SN Name** | **Observation Date (MM-DD-YYYY)** | **Days Since Discovery** | **Discovery Date (MJD)** | **Count Rate (photons/s)** | **(+) Rate Error (photons/s)** | **(-) Rate Error (photons/s)** | **Luminosity (ergs/s)** |
|---|---|---|---|---|---|---|---|
| SN2018aoq | 04-04-2016 | 1.288 | 58209 | 5.8631e-02 | +5.2120e-03 | -5.2120e-03 | 1.41536e+41 |
| SN2018ivc | 08-10-2017 | 0.3513 | 58446 | 7.405e-02 | +3.241e-02 | -3.241e-02 | 5.06159e+41 |
| SN2018lei | 01-13-2019 | 4.23 | 58483 | 7.028682e-03 | +3.475776e-03 | -2.638357e-03 | 5.7759e+39 |
| SN2019bl | 01-17-2019 | 5.94 | 58485 | 2.284620e-03 | +1.327107e-03 | -9.802035e-04 | 1.9659e+40 |

## 3.2 Plots

### *3.2.1 Sample Plot of Luminosity vs. Time*

**Figure 3.1** shown below displays the resulting plot of upper limits for luminosity in ergs/s versus time in days since detection for SN2018hna from the python codes in **Figure 2.1** and **Figure 2.2**.

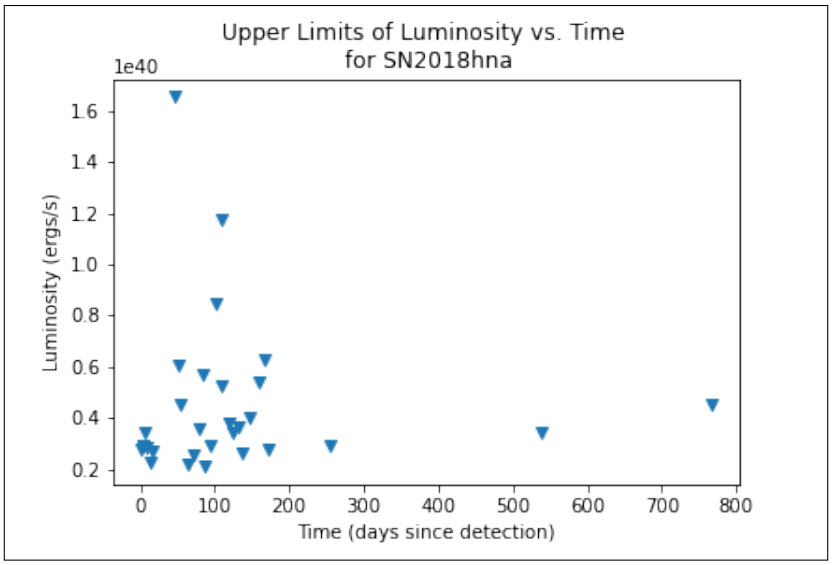


Figure 3.1: Plotting Luminosity Upper Limits vs. Time

### *3.2.2 Overlaid Plot of Luminosity vs. Time*

**Figure 3.2** shown below displays the resulting plot of luminosity versus time since detection for all 18 supernovae from the python code in **Figure 2.3**. Note that negative time values indicate observations made prior to explosion. Also note that SN2018aoq's host galaxy has a bright luminosity, meaning Swift has a hard time detecting the X-rays from the supernova itself, and most detected X-rays were likely from the host galaxy.

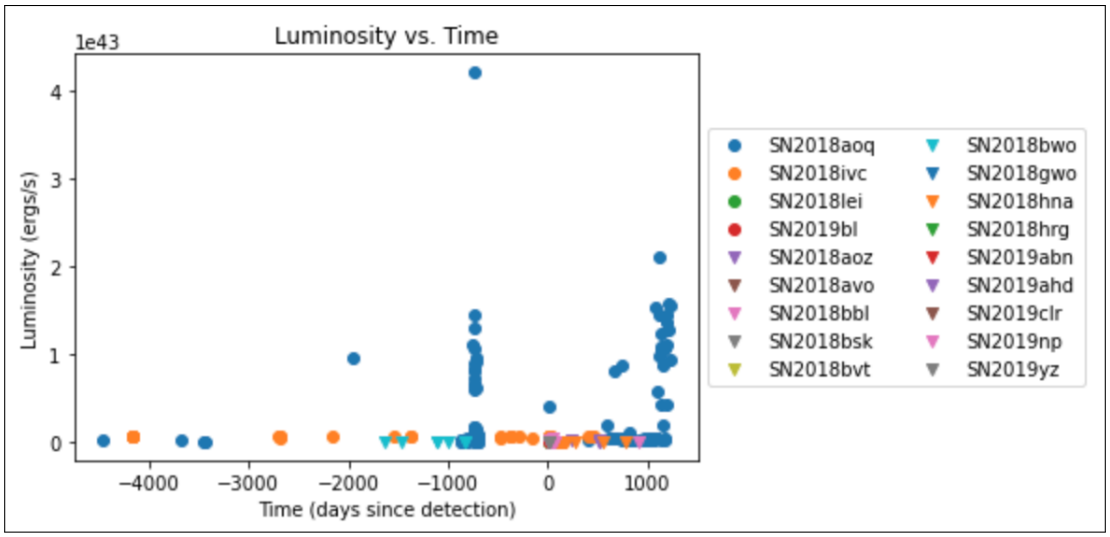


Figure 3.2: Overlaid Plot of Luminosity vs. Time for 18 SN

### *3.2.3 Plot of Detected Luminosity vs. Time*

**Figure 3.3** shown below displays the resulting plot of luminosity versus time since detection for the 4 supernovae with detections after eliminating the lines of code containing supernovae with only upper limits from the Python code in **Figure 2.3**. Individual plots of each supernova can be found in **Appendix A: Plots** at the end of this paper, excluding SN2019bl, which only had one detection. Note that negative time values indicate observations made prior to explosion and are likely from the host galaxy rather than the supernova, but it is unclear how drastically this affects the data.

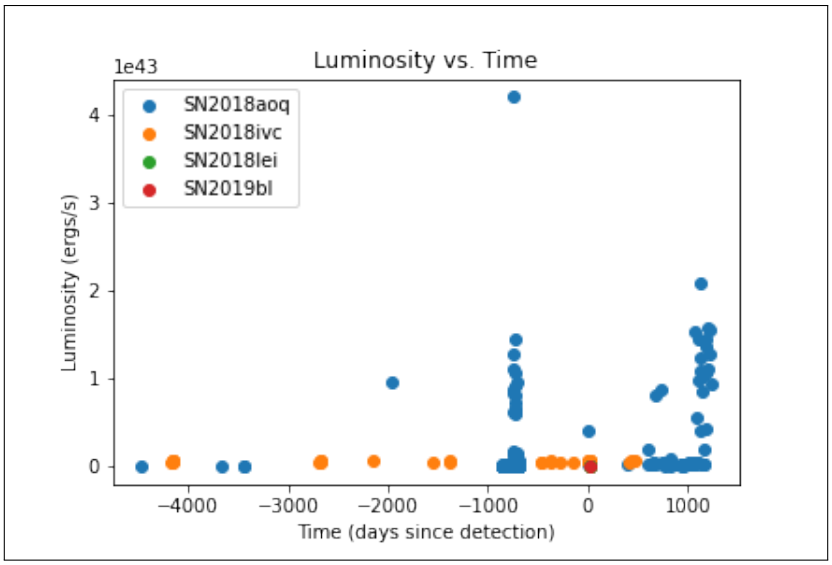


Figure 3.3: Plot of Luminosity vs. Time for the 4 SN with Detections

### *3.2.4 Plot of Luminosity Upper Limits*

**Figure 3.4** contains upper limits for luminosity for 14 supernovae. For legibility, only observations made from zero to five days after detection were included.

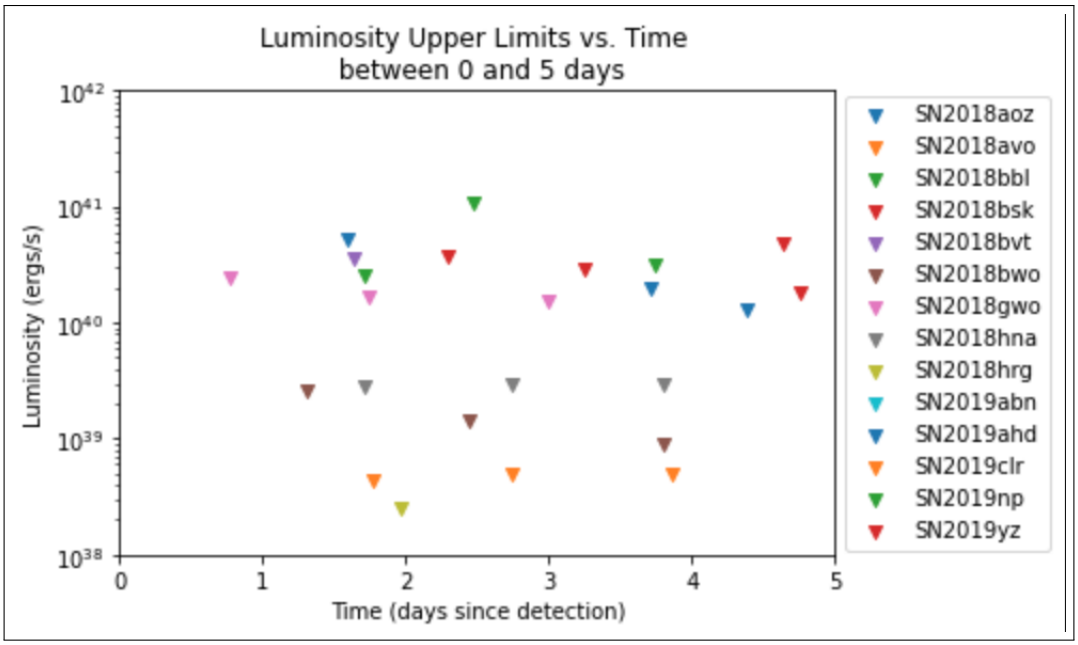


Figure 3.4: Plot of Luminosity Upper Limits vs. Time Between 0-5 Days

### *3.2.5 Remaining Luminosity vs. Time Plots*

Plots of luminosity versus time for SN2018aoq, SN2018aoz, SN2018bbl, SN2018bsk, SN2018bwo, SN2019clr, SN2018gwo, SN2018ivc, SN2018lei, SN2019abn, SN2019ahd, SN2019np, and SN2019yz can be found in **Appendix A: Plots** at the end of this paper. Note that SN2018avo, SN2018bvt, SN2018hrg, and SN2019bl were observed but not plotted, as they each only contained one data point. Also note that the plots of SN2018aoq, SN2018bwo, and SN2018ivc contain the error bars associated with each data point.

### *3.2.6 GRB060218*

GRB060218, also known as SN2006aj, is a unique case of a supernova being discovered using X-ray detections. A detailed plot of detected luminosity versus time for GRB060218 was generated using the Swift-XRT Products Generator, with binning set to constant counts per bin, and also with information from [24]. The count rates were converted to fluxes using part of the code seen in **Figure 2.1**, and the times were converted from units of seconds to days since de-

tection using the code in **Figure 2.2**. The resulting curve can be seen in **Figure 3.5**. This curve was created to compare detected data for X-ray emissions to the data for upper limits to determine how constraining our upper limits were. The plot showing this comparison, with the y-axis set to a logarithmic scale and time values limited to between zero and five days since detection, can be seen in **Figure 3.6**. From the comparison plot, it can be seen that the upper limits on luminosity fall slightly under the detected GRB, which means we can rule out long-lasting emission of comparable luminosity. This also shows that the upper limits are sensitive enough and likely show detections for the respective supernovae. These observations are sensitive enough to indicate possible detections, but some need to be made sooner to constrain the early shock breakout emission, which would be made possible using SIBEX.

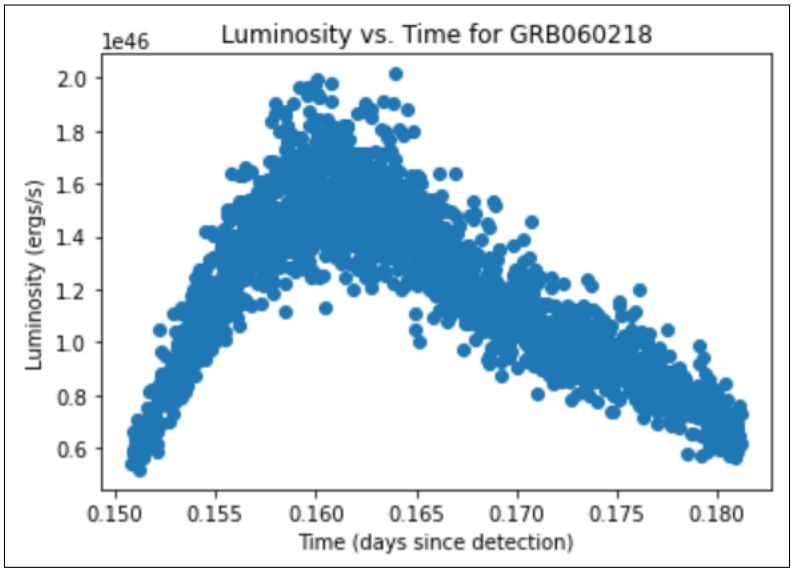


Figure 3.5: Light Curve of GRB060218

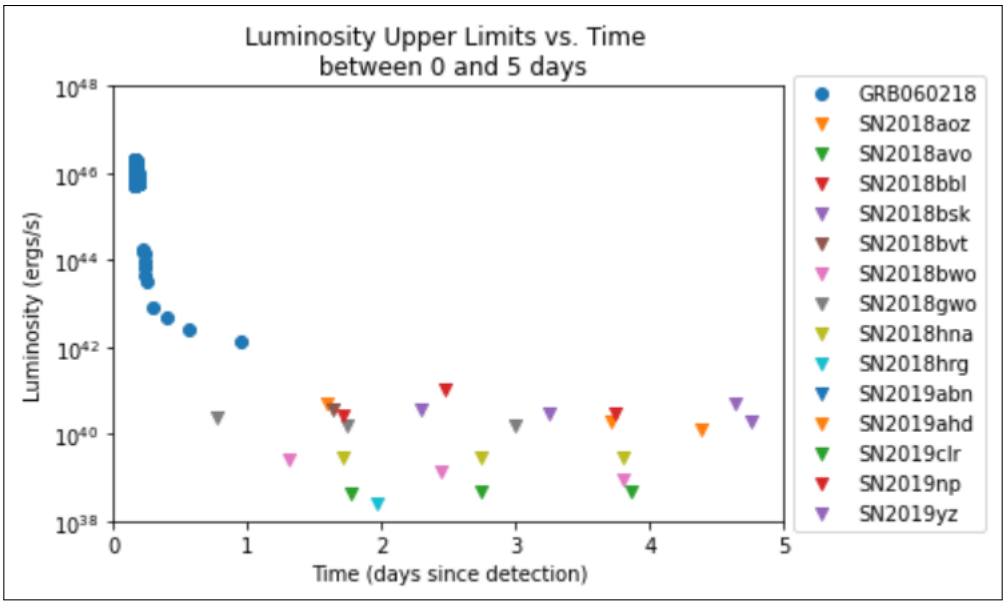


Figure 3.6: Comparison of GRB060218 to Upper Limits of 14 SN

### *3.2.7 SN2018ivc*

**Figure 3.7** shows X-ray images of the field of SN2018ivc before and immediately after explosion in the optical and X-ray light, with the location of SN2018ivc marked with a green circle with a radius of 15 arcseconds. **Figure 3.8** shows SN2018ivc after explosion. X-rays from the supernova are clearly visible in the images after explosion, but it is difficult to subtract off the background X-rays from the galaxy. This is also the case for SN2018aoq and SN2018bwo. As previously mentioned, this background interference makes it difficult to interpret the XRT data for these supernovae.

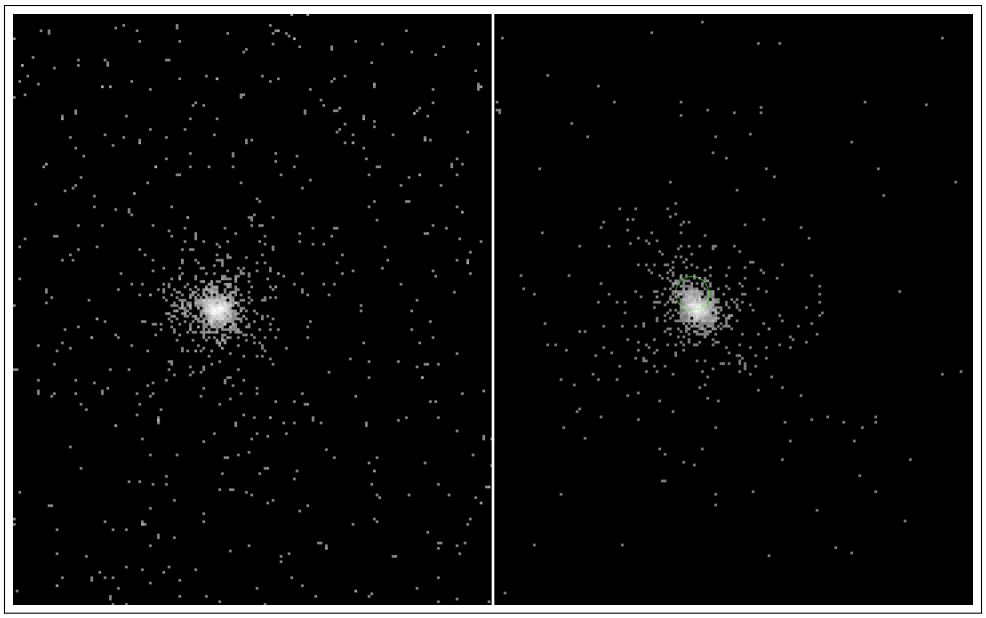

Figure 3.7: X-Ray Images of SN2018ivc's Field Before (Left) and Immediately After (Right) Explosion
(Images from P. Brown, Private Communication)

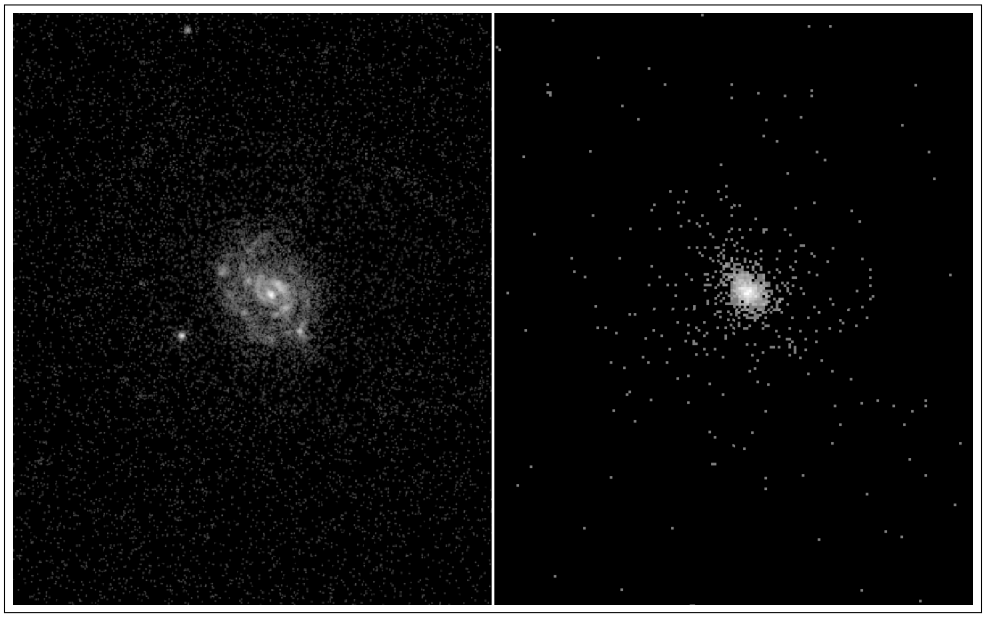

Figure 3.8: Optical/UVOT (Left) and X-Ray (Right) Images of SN2018ivc's Host Galaxy
(Images from P. Brown, Private Communication)

# 4. CONCLUSION

## 4.1 Detection Rates

Of the 18 supernovae that were reviewed, only 3 had confirmed detections, as it was decided that SN2019bl was not actually a supernova. The formally detected supernovae, which are SN2018aoq, SN2018ivc, and SN2018lei, showed a high galaxy brightness and pre-explosion detections, which suggest that the detections are from the galaxy rather than the supernova. The upper limits for the remaining 14 supernovae that were not formally detected are seen to be lower than the detections of GRB060218/SN2006aj, which suggests that at low levels of galaxy contamination, the XRT is sensitive enough to make detections. However, the small amount of detections places a constraint on the number of supernovae that could be that luminous. The detections made through these analyses will help in future observations by setting a precedent for expected results and by being used to make comparisons between theoretical and actual data, which will help SIBEX to make detections at the moment of explosion.

## 4.2 SIBEX

The resulting data from observing these supernovae will be very helpful in calibrating the future telescope system SIBEX. By viewing how the proposed upper limits compared to physical data, we can learn to better constrain some of the physics of the explosion. In the future, this will allow us to compare SIBEX's sensitivity to that which is necessary for detections to be made, which will cause the supernovae to be detected at the moment of explosion and give more useful data. Gathering better data will help us to be able to distinguish between X-rays emitted by host galaxies and those emitted by a supernova itself, which will make observations more clear and understandable and results more conclusive.

# REFERENCES


[1] Harvard, "Supernovas & supernova remnants," May 2013.

[2] Harvard, "X-rays- another form of light," May 2012.

[3] R. Nave, "Compton scattering."

[4] S. Chakraborti, A. Ray, R. Smith, R. Margutti, D. Pooley, S. Bose, F. Sutaria, P. Chandra, V. V. Dwarkadas, S. Ryder, and K. Maeda, "Probing final stages of stellar evolution with x-ray observations of sn 2013ej," 2015.

[5] E. M. Schlegel, "X-ray emission from supernovae: a review of the observations," *Reports on Progress in Physics*, vol. 58, pp. 1375–1413, Nov. 1995.

[6] H. U. Zimmermann, W. Lewin, P. Predehl, B. Aschenbach, G. Fabbiano, G. Hasinger, L. Lubin, E. Magnier, J. van Paradijs, R. Petre, W. Pietsch, and J. Trümper, "Detection of soft X-rays from supernova 1993J six days after outburst," , vol. 367, pp. 621–623, Feb. 1994.

[7] K. A. Bostroem, S. Valenti, D. J. Sand, J. E. Andrews, S. D. Van Dyk, L. Galbany, D. Pooley, R. C. Amaro, N. Smith, S. Yang, G. C. Anupama, I. Arcavi, E. Baron, P. J. Brown, J. Burke, R. Cartier, D. Hiramatsu, R. Dastidar, J. M. DerKacy, Y. Dong, E. Egami, S. Ertel, A. V. Filippenko, O. D. Fox, J. Haislip, G. Hosseinzadeh, D. A. Howell, A. Gangopadhyay, S. W. Jha, V. Kouprianov, B. Kumar, M. Lundquist, D. Milisavljevic, C. McCully, P. Milne, K. Misra, D. E. Reichart, D. K. Sahu, H. Sai, A. Singh, P. S. Smith, J. Vinko, X. Wang, Y. Wang, J. C. Wheeler, G. G. Williams, S. Wyatt, J. Zhang, and X. Zhang, "Discovery and Rapid Follow-up Observations of the Unusual Type II SN 2018ivc in NGC 1068," , vol. 895, p. 31, May 2020.

[8] A. Nisenoff, V. V. Dwarkadas, and M. C. Ross, "Supernova x-ray database (SNaX) updated to ensure long-term stability," *Research Notes of the AAS*, vol. 4, p. 195, nov 2020.

[9] S. F. Hönig, D. Watson, M. Kishimoto, and J. Hjorth, "A dust-parallax distance of 19 megaparsecs to the supermassive black hole in NGC 4151," , vol. 515, pp. 528–530, Nov. 2014.

[10] R. B. Tully, H. M. Courtois, A. E. Dolphin, J. R. Fisher, P. Héraudeau, B. A. Jacobs, I. D. Karachentsev, D. Makarov, L. Makarova, S. Mitronova, L. Rizzi, E. J. Shaya, J. G. Sorce, and P.-F. Wu, "Cosmicflows-2: The Data," , vol. 146, p. 86, Oct. 2013.

[11] L. Bottinelli, L. Gouguenheim, G. Paturel, and P. Teerikorpi, "The Malmquist bias and the value of H zero from the Tully-Fisher relation.," , vol. 156, pp. 157–171, Feb. 1986.

[12] R. B. Tully and J. R. Fisher, *Catalog of Nearby Galaxies*. 1988.

[13] N. Yasuda, M. Fukugita, and S. Okamura, "Study of the Virgo Cluster Using the B-Band Tully-Fisher Relation," , vol. 108, pp. 417–448, Feb. 1997.

[14] E. Sabbi, D. Calzetti, L. Ubeda, A. Adamo, M. Cignoni, D. Thilker, A. Aloisi, B. G. Elmegreen, D. M. Elmegreen, D. A. Gouliermis, E. K. Grebel, M. Messa, L. J. Smith, M. Tosi, A. Dolphin, J. E. Andrews, G. Ashworth, S. N. Bright, T. M. Brown, R. Chandar, C. Christian, G. C. Clayton, D. O. Cook, D. A. Dale, S. E. de Mink, C. Dobbs, A. S. Evans, M. Fumagalli, I. Gallagher, J. S., K. Grasha, A. Herrero, D. A. Hunter, K. E. Johnson, L. Kahre, R. C. Kennicutt, H. Kim, M. R. Krumholz, J. C. Lee, D. Lennon, C. Martin, P. Nair, A. Nota, G. Östlin, A. Pellerin, J. Prieto, M. W. Regan, J. E. Ryon, E. Sacchi, D. Schaerer, D. Schiminovich, F. Shabani, S. D. Van Dyk, R. Walterbos, B. C. Whitmore, and A. Wofford, "The Resolved Stellar Populations in the LEGUS Galaxies1," , vol. 235, p. 23, Mar. 2018.

[15] G. Theureau, M. O. Hanski, N. Coudreau, N. Hallet, and J. M. Martin, "Kinematics of the Local Universe. XIII. 21-cm line measurements of 452 galaxies with the Nançay radiotelescope, JHK Tully-Fisher relation, and preliminary maps of the peculiar velocity field," , vol. 465, pp. 71–85, Apr. 2007.

[16] I. D. Karachentsev, D. I. Makarov, and E. I. Kaisina, "Updated Nearby Galaxy Catalog," , vol. 145, p. 101, Apr. 2013.

[17] M. G. Lee and I. S. Jang, "Dual Stellar Halos in the Standard Elliptical Galaxy M105 and Formation of Massive Early-type Galaxies," , vol. 822, p. 70, May 2016.

[18] O. G. Nasonova, J. A. de Freitas Pacheco, and I. D. Karachentsev, "Hubble flow around Fornax cluster of galaxies," , vol. 532, p. A104, Aug. 2011.

[19] D. G. Russell, "The H I Line Width/Linear Diameter Relationship as an Independent Test of the Hubble Constant," , vol. 565, pp. 681–695, Feb. 2002.

[20] I. D. Karachentsev, O. G. Nasonova, and V. E. Karachentseva, "Large-scale structure and galaxy motions in the Leo/Cancer constellations," *Astrophysical Bulletin*, vol. 70, pp. 1–15, Jan. 2015.

[21] R. B. Tully, H. M. Courtois, and J. G. Sorce, "Cosmicflows-3," , vol. 152, p. 50, Aug. 2016.

[22] W. L. Freedman, B. F. Madore, B. K. Gibson, L. Ferrarese, D. D. Kelson, S. Sakai, J. R. Mould, J. Kennicutt, Robert C., H. C. Ford, J. A. Graham, J. P. Huchra, S. M. G. Hughes, G. D. Illingworth, L. M. Macri, and P. B. Stetson, "Final Results from the Hubble Space Telescope Key Project to Measure the Hubble Constant," , vol. 553, pp. 47–72, May 2001.

[23] S. Immler, P. J. Brown, P. Milne, L. S. The, R. Petre, N. Gehrels, D. N. Burrows, J. A. Nousek, C. L. Williams, E. Pian, P. A. Mazzali, K. Nomoto, R. A. Chevalier, V. Mangano, S. T. Holland, P. W. A. Roming, J. Greiner, and D. Pooley, "X-Ray Observations of Type Ia Supernovae with Swift: Evidence of Circumstellar Interaction for SN 2005ke," , vol. 648, pp. L119–L122, Sept. 2006.

[24] S. Campana, V. Mangano, A. J. Blustin, P. Brown, D. N. Burrows, G. Chincarini, J. R. Cummings, G. Cusumano, M. D. Valle, D. Malesani, P. Mészáros, J. A. Nousek, M. Page, T. Sakamoto, E. Waxman, B. Zhang, Z. G. Dai, N. Gehrels, S. Immler, F. E. Marshall, K. O. Mason, A. Moretti, P. T. O'Brien, J. P. Osborne, K. L. Page, P. Romano, P. W. A. Roming, G. Tagliaferri, L. R. Cominsky, P. Giommi, O. Godet, J. A. Kennea, H. Krimm, L. Angelini, S. D. Barthelmy, P. T. Boyd, D. M. Palmer, A. A. Wells, and N. E. White, "The association of grb 060218 with a supernova and the evolution of the shock wave," *Nature*, vol. 442, p. 1008–1010, Aug 2006.

# APPENDIX A: PLOTS

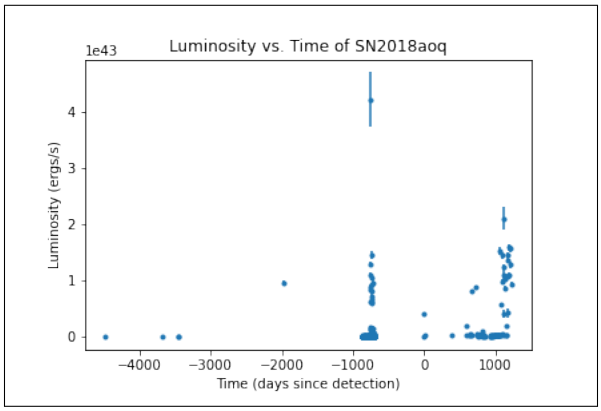


Figure A.1: Plot of Luminosity vs. Time for SN2018aoq with Error Bars

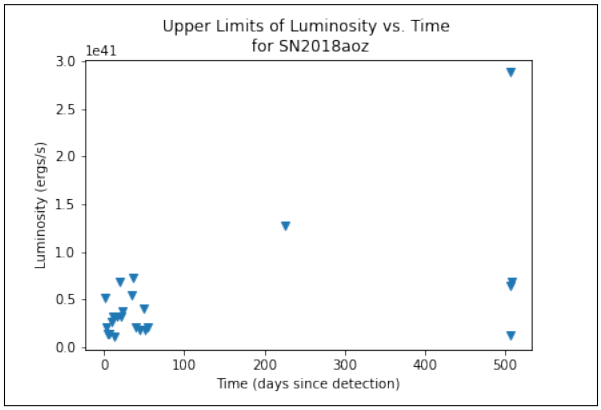


Figure A.2: Plot of Upper Limits of Luminosity vs. Time for SN2018aoz

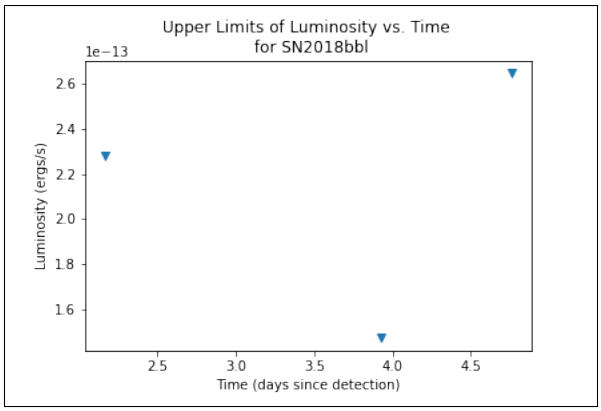


Figure A.3: Plot of Upper Limits of Luminosity vs. Time for SN2018bbl

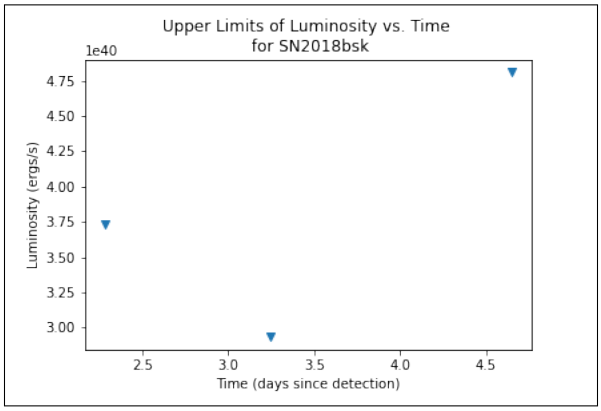


Figure A.4: Plot of Upper Limits of Luminosity vs. Time for SN2018bsk

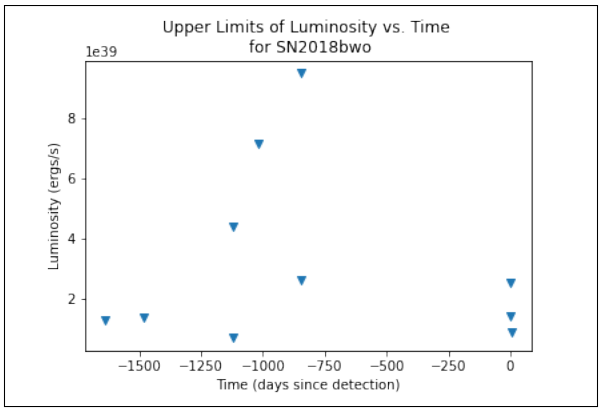


Figure A.5: Plot of Upper Limits of Luminosity vs. Time for SN2018bwo

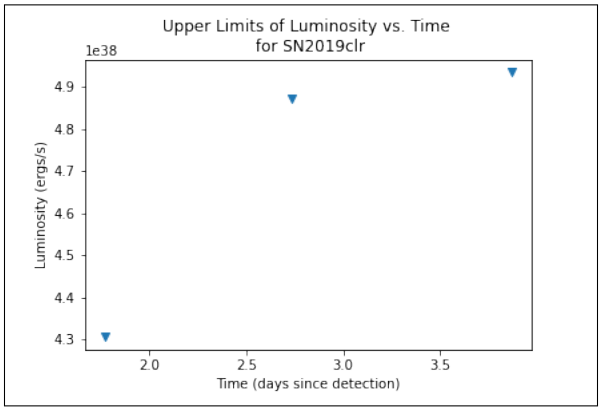


Figure A.6: Plot of Upper Limits of Luminosity vs. Time for SN2019clr

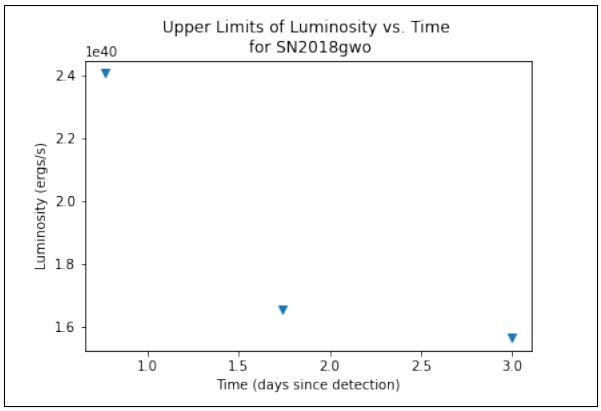


Figure A.7: Plot of Upper Limits of Luminosity vs. Time for SN2018gwo

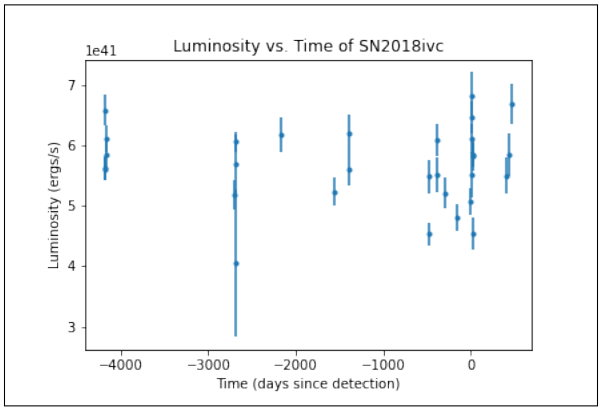


Figure A.8: Plot of Luminosity vs. Time for SN2018ivc with Error Bars

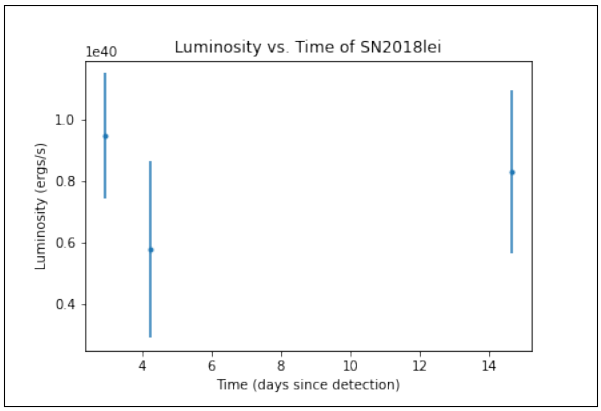


Figure A.9: Plot of Luminosity vs. Time for SN2018lei with Error Bars

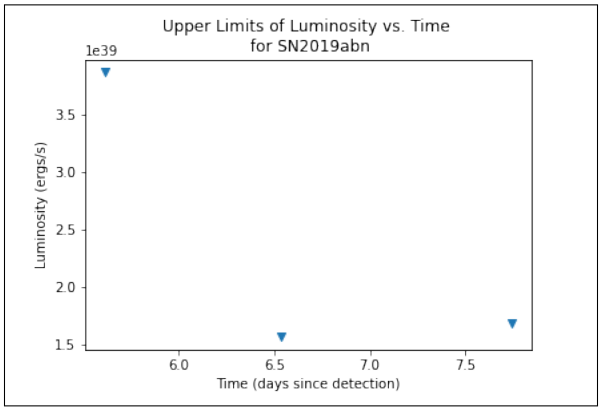


Figure A.10: Plot of Upper Limits of Luminosity vs. Time for SN2019abn

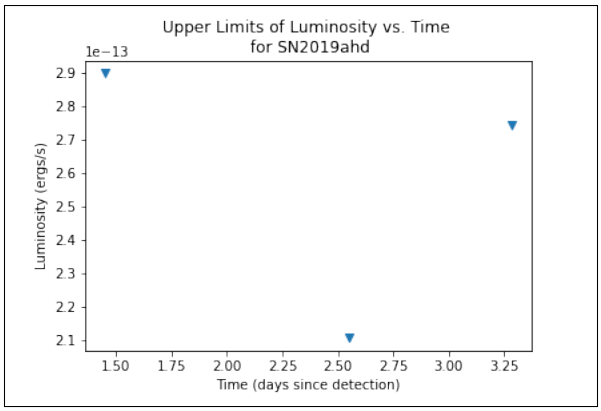


Figure A.11: Plot of Upper Limits of Luminosity vs. Time for SN2019ahd

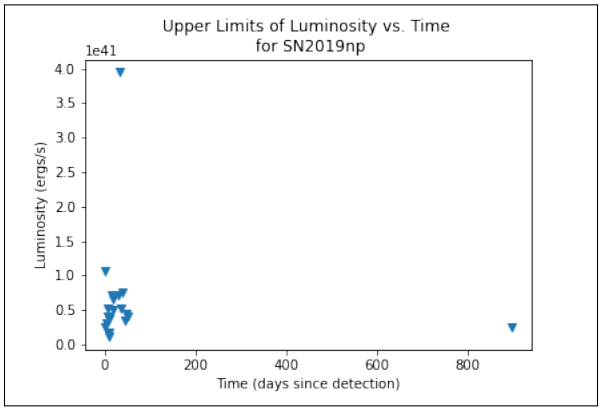


Figure A.12: Plot of Upper Limits of Luminosity vs. Time for SN2019np

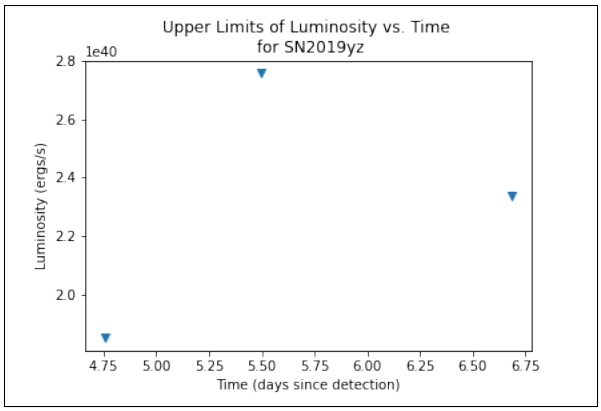


Figure A.13: Plot of Upper Limits of Luminosity vs. Time for SN2019yz